

## DESIGN CHANGE AND FEASIBILITY ANALYSIS OF SALUS REACTOR INTERNAL STRUCTURES

Jong-Bum Kim<sup>a\*</sup>, Chang-Gyu Park<sup>a</sup>

<sup>a</sup>Korea Atomic Energy Research Institute, Daedeok-daero 989, Yuseong-gu, Daejeon, Korea

\*Corresponding Author: jbkim@kaeri.re.kr

### 1. Introduction

The conceptual design of the Generation-IV advanced small reactor SALUS (Small, Advanced, Long-cycled and Ultimate Safe SFR)[1] has been under development and it is based upon the structural concept and design specifications of the PGSFR[2], but adopts a long-term reactor core. The preliminary structural design was carried to ensure integrity against the design loads to meet the long-term core and thermal fluid requirements.

In this study, the shape and dimensions of the SALUS reactor internal structures were changed from those of PGSFR, and the feasibility was analyzed by evaluating the structural integrity against the design condition loadings.

### 2. Design of SALUS Reactor Internal Structures

The reactor internal structures of PGSFR consist of core support structure, inlet plenum, core shroud, IVS shroud, separation plate, redan structure, and UIS as shown in Fig. 1. The redan structure is a single integrated unit that separates the hot pool from cold pool and it consists of multiple plates welded together that form a contoured shape around IHXs and UIS. The IHXs are located within the redan but the primary pumps and DHXs are located outside the redan in the cold pool. Thus, the redan became a peanut-shaped structure[3].

The major functions of the reactor internal structures are to provide the location of main components inside the reactor vessel, to support the load of the reactor structures such as the reactor core, shields and internal pipes, to protect the core from external loads, and to provide the thermal boundary of the hot pool and cold pool sodium coolant.

The SALUS with a long-term core promoted to accommodate the structural concept of the PGSFR as far as possible and to make some design changes if necessary. The reactor vessel and containment vessel reflected a slight increase in the length of the core and a change in the cold pool liquid level, and the reactor support structure was improved to relieve thermal stress by directly supporting the reactor vessel on the reactor head. On the other hand, the reactor internal structures of SALUS have been significantly changed to improve the structural integrity. A complex peanut-shaped redan structure was changed to a simple cylindrical upper inner vessel and a horizontal separation plate was changed to a conical middle inner vessel as shown in Fig. 2. Support cylinders for main components are welded upward to the middle inner vessel, and the DHX and pump are positioned therein to be basically installed in the cold pool. The core support structure has a skirt shape and is welded to the lug installed on the core support flange of the lower head of the reactor vessel, and the concept of the PGSFR is applied as it is.

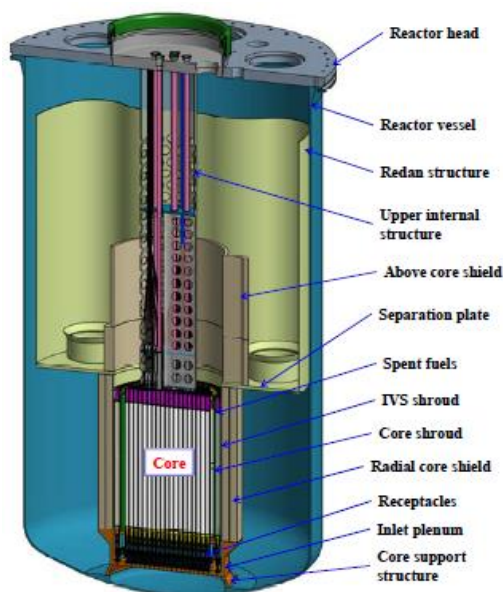


Fig. 1 Reactor vessel and internal structures (PGSFR)

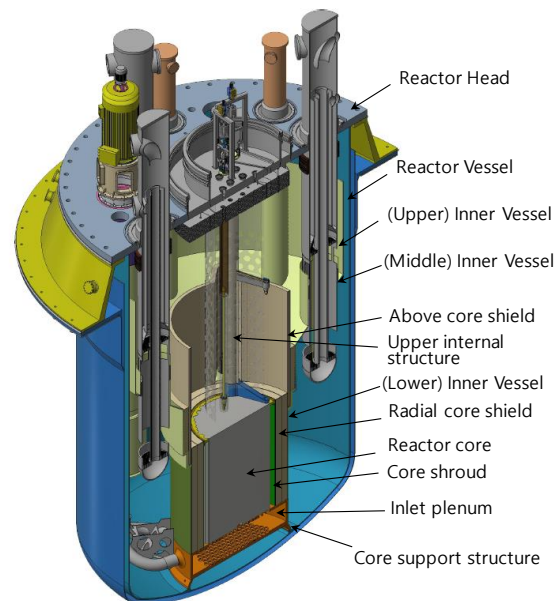


Fig. 2 Reactor vessel and internal structures (SALUS)

### 3. Structural Integrity Assessment of SALUS Reactor Internal Structures

Structural analysis was performed for the SALUS reactor internal structures with respect to the design condition loadings and the structural integrity assessment was carried out per ASME B&PV Code, Section III, Division 5[4]. While a maximum operating temperature is 510°C, design temperatures of hot and cold pools are applied as 520°C and 360°C, respectively.

#### Structural analysis model

ANSYS Version 2019[5] was used for a finite element analysis to evaluate the structural analysis of the reactor internal structures, and an analysis model was prepared as a half symmetrical model considering the symmetry of the structure. All the reactor internal structures are made of Type 316 Stainless Steel and its material properties are shown in Table 1. It is assumed that the physical properties of the core shielding structure are the same as that of the structural material Type 316SS, and only the density is set to 70% of the Type 316SS.

Table 1. Material properties of Type 316 Stainless steel

| Tem p. (°C) | Thermal Conductivity (W/(m°C)) | Thermal Expansion (Sequent) (m/m/°C) × 10 <sup>-6</sup> | Specific Heat (J/(kg°C)) | Elastic Modulus (GPa) | Density (kg/m <sup>3</sup> ) | Poisson's Ratio |
|-------------|--------------------------------|---|--------------------------|-----------------------|------------------------------|-----------------|
| 20          | 14.1                           | 15.3  | 491.9                    | 195                   | 8030                         | 0.31            |
| 100         | 15.4                           | 16.2  | 511.4                    | 189                   | 8030                         | 0.31            |
| 200         | 16.8                           | 17.0  | 525.7                    | 183                   | 8030                         | 0.31            |
| 300         | 18.3                           | 17.7  | 540.0                    | 176                   | 8030                         | 0.31            |
| 400         | 19.7                           | 18.1  | 552.5                    | 169                   | 8030                         | 0.31            |
| 500         | 21.2                           | 18.4  | 566.5                    | 160                   | 8030                         | 0.31            |
| 600         | 22.6                           | 18.8  | 574.4                    | 151                   | 8030                         | 0.31            |

Figure 3 shows a finite element analysis model of the reactor internal structures. The element used for the analysis was Solid185 (3D 8-node structural solid) element and the total number of elements and nodes are 105,076 and 153,169, respectively.

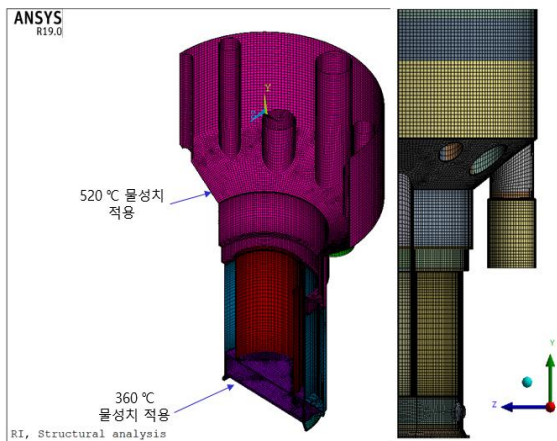


Fig. 3 Finite element model of reactor internal structures

Design condition loadings are dead weights of reactor internal structures, reactor cores and shielding structures, and sodium coolant hydraulic pressure (sodium density of 903 kg/m<sup>3</sup> at 204 °C).

#### Structural analysis result

Figure 4 shows the stress distribution as a result of structural analysis of the reactor internal structures against design condition loadings. It can be seen that the maximum stress intensity (64.6 MPa) occurred at the lower key of the core support.

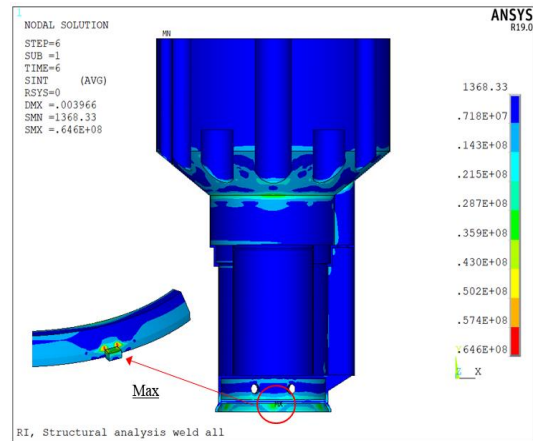


Fig. 4 Stress intensity distribution of reactor internal structures

One of the important areas in the reactor internal structures is an inner vessel. Large stress intensity (57.3 MPa) occurred at the connection region of the support cylinder for primary pump in the middle inner vessel as shown in Fig. 5.

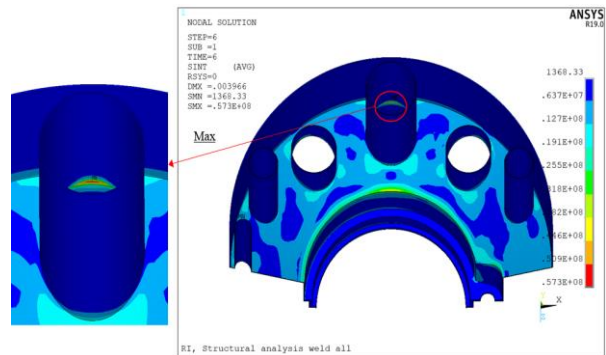


Fig. 5 Stress intensity distribution in inner vessel

#### Structural integrity assessment

Based upon the results of the structural analysis, the structural integrity was evaluated for the reactor internal structures according to the ASME B&PV Code, Section III, Division 5. As described in the previous section, the lower key of the core support where the maximum stress intensity occurred and the connection region of the middle inner vessel were selected for their structural integrity assessment.

##### (a) Core support

The maximum stress intensity was generated at the lower key of the core support structure, and the two cross sections (Cut A and Cut B) were selected for structural integrity assessment as shown in Fig. 6 and

the stress linearization was carried out. The structural integrity was assessed per ASME B&PV Code, Section III, Division 5.

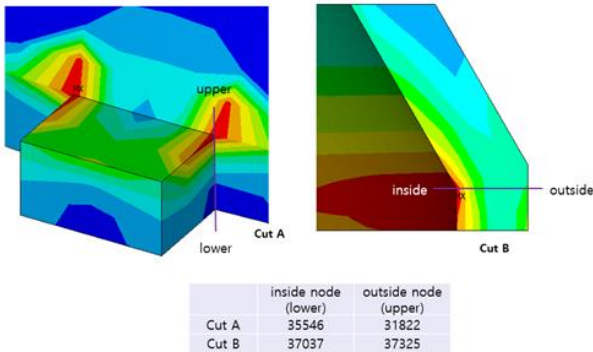


Fig. 6 Assessment sections of core support structure

Table 2 summarizes the structural integrity evaluation results for Cut A and Cut B, which are the main cross-sections of core supports. As shown in Table 2, it can be seen that the design margin on each section is larger than 300% and it was confirmed that the structural integrity was secured sufficiently.

Table 2. Structural integrity assessment results of core support structure

| Section | Nodes | Linearized Stress | Calculated Stress(MPa) | Allowable Stress (Mpa) | Margin | Temperature (°C) | C&S                               |
|---------|-------|-------------------|------------------------|------------------------|--------|------------------|-----------------------------------|
| Cut A   | Inner | $P_m$             | 15.5                   | $S_{m,1} = 113.2$      | 6.3    | 360              | ASME Sec III Div. 5 Sec II Part D |
|         |       | $P_L$             | 15.5                   | $1.5S_{m,1} = 169.8$   | 10.0   | 360              | ASME Sec III Div. 5 Sec II Part D |
|         |       | $P_L + P_b$       | 17.4                   | $1.5S_{m,1} = 169.8$   | 8.8    | 360              | ASME Sec III Div. 5 Sec II Part D |
|         | Outer | $P_m$             | 15.5                   | $S_{m,2} = 113.2$      | 6.3    | 360              | ASME Sec III Div. 5 Sec II Part D |
|         |       | $P_L$             | 15.5                   | $1.5S_{m,2} = 169.8$   | 10     | 360              | ASME Sec III Div. 5 Sec II Part D |
|         |       | $P_L + P_b$       | 42.8                   | $1.5S_{m,2} = 169.8$   | 3.0    | 360              | ASME Sec III Div. 5 Sec II Part D |
| Cut B   | Inner | $P_m$             | 9.4                    | $S_{m,1} = 113.2$      | 11.0   | 360              | ASME Sec III Div. 5 Sec II Part D |
|         |       | $P_L$             | 9.4                    | $1.5S_{m,1} = 169.8$   | 17.1   | 360              | ASME Sec III Div. 5 Sec II Part D |
|         |       | $P_L + P_b$       | 20.2                   | $1.5S_{m,1} = 169.8$   | 7.4    | 360              | ASME Sec III Div. 5 Sec II Part D |
|         | Outer | $P_m$             | 9.4                    | $S_{m,2} = 113.2$      | 11.0   | 360              | ASME Sec III Div. 5 Sec II Part D |
|         |       | $P_L$             | 9.4                    | $1.5S_{m,2} = 169.8$   | 17.1   | 360              | ASME Sec III Div. 5 Sec II Part D |
|         |       | $P_L + P_b$       | 14.6                   | $1.5S_{m,2} = 169.8$   | 10.6   | 360              | ASME Sec III Div. 5 Sec II Part D |

(b) Inner vessel

Large stress intensity occurred at the connection region of the middle inner vessel and the support cylinder for IHX, and the two specific cross sections (Cut C and Cut D) were selected for structural integrity assessment as shown in Fig. 7. Stress linearization was carried out and Table 3 summarizes the structural integrity evaluation results against design condition loadings.

Table 3 shows that the design margin for each cross-section is more than 190% which is quite larger than the target design margin. Thus, it was confirmed that the structural integrity of the middle inner vessel is secured with sufficient design margin.

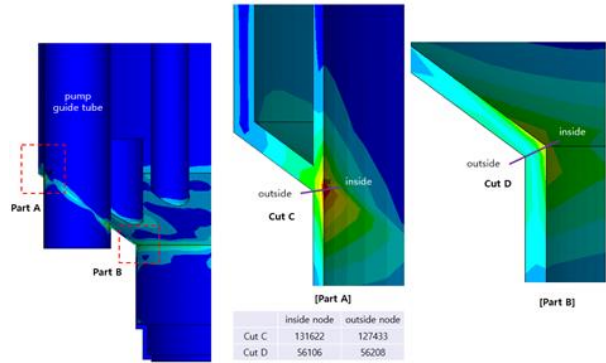


Fig. 7 Assessment sections of middle inner vessel

Table 3. Structural integrity assessment results of inner vessel

| Section | Nodes | Linearized Stress | Calculated Stress(MPa) | Allowable Stress (Mpa) | Margin | Temperature (°C) | C&S                 |
|---------|-------|-------------------|------------------------|------------------------|--------|------------------|---------------------|
| Cut C   | Inner | $P_m$             | 35.5                   | $S_{m,1} = 105.2$      | 2.0    | 520              | ASME Sec III Div. 5 |
|         |       | $P_L$             | 35.5                   | $1.5S_{m,1} = 157.8$   | 3.4    | 520              | ASME Sec III Div. 5 |
|         |       | $P_L + P_b$       | 55.3                   | $1.5S_{m,1} = 157.8$   | 1.9    | 520              | ASME Sec III Div. 5 |
|         | Outer | $P_m$             | 35.5                   | $S_{m,2} = 105.2$      | 2.0    | 520              | ASME Sec III Div. 5 |
|         |       | $P_L$             | 35.5                   | $1.5S_{m,2} = 157.8$   | 3.4    | 520              | ASME Sec III Div. 5 |
|         |       | $P_L + P_b$       | 30.6                   | $1.5S_{m,2} = 157.8$   | 4.2    | 520              | ASME Sec III Div. 5 |
| Cut D   | Inner | $P_m$             | 21.0                   | $S_{m,1} = 105.2$      | 4.0    | 520              | ASME Sec III Div. 5 |
|         |       | $P_L$             | 21.0                   | $1.5S_{m,1} = 157.8$   | 6.5    | 520              | ASME Sec III Div. 5 |
|         |       | $P_L + P_b$       | 37.3                   | $1.5S_{m,1} = 157.8$   | 3.2    | 520              | ASME Sec III Div. 5 |
|         | Outer | $P_m$             | 21.0                   | $S_{m,2} = 105.2$      | 4.0    | 520              | ASME Sec III Div. 5 |
|         |       | $P_L$             | 21.0                   | $1.5S_{m,2} = 157.8$   | 6.5    | 520              | ASME Sec III Div. 5 |
|         |       | $P_L + P_b$       | 19.2                   | $1.5S_{m,2} = 157.8$   | 7.2    | 520              | ASME Sec III Div. 5 |

#### 4. Results and Discussion

The design of the reactor internal structures of SALUS has been changed from those of PGSFR and the feasibility was analyzed by performing the corresponding structural integrity assessment.

Structural analysis of the reactor internal structures subjected to the design condition loadings and the corresponding structural integrity assessment according to the ASME B&PV Code, Sec. III, Division 5 were carried out. The results show that the reactor internal structure was found to satisfy the design limit with a sufficient margin under the design conditions in all parts.

#### Acknowledgement

This work was supported by a grant from the National Research Foundation of Korea (NRF) funded by the Korean government (Ministry of Science and ICT) (NRF-2021M2E2A1037872).

#### REFERENCES

- [1] J.H. Lee, Design Basis for SALUS, SAL-010-E3-402-002, KAERI, 2022
- [2] System description of SFR prototype reactor, SFR-000-P-403-001, 2015.
- [3] C.G. Park, G.H. Koo, J.H. Cho and S.K. Kim, "Mechanical Design Features of PGSFR NSSS," Transactions of the Korean Nuclear Society Spring Meeting, Korea, 2016.
- [4] ASME Boiler and Pressure Vessel Code, Section III, Division 5, 2017.
- [5] ANSYS Users Manual, Release 2019, ANSYS Inc., 2019.